EARTH SCIENCES
RESEARCH JOURNAL

Earth Sci. Res. J. Vol. 23, No. 1 (March, 2019): 17-25

UNIVERSIDAD NACIONAL DE COLOMBIA

GEOLOGY

Determination of Distance Required to Ensure Stope and Footwall-drift Non-interaction Zone based on Geological Strength Index

Mehmet Volkan Ozdogan, Alper Gonen
Dokuz Eylul University Engineering Faculty Department Of Mining Engineering.
* Corresponding author: mehmet.ozdogan@deu.edu.tr

ABSTRACT

In the Bakibaba Copper Mine, the longhole stoping method is used in the production of copper ore. Stability problems have occurred at times on the footwall drift due to the interaction between the footwall drift and stope. In this study, we propose a method for estimating the minimum distance necessary to ensure a non-interaction zone between the footwall drift and stope. We used the finite element method and various distances between the footwall drift and stope and the displacements over drifts as parameters. We also performed analyses on various geological strength index values from low to high to determine the effect of the rock mass on the interaction between the footwall drift and stope.

Keywords: Footwall drift, numerical analysis, underground stability.

Determinación de la distancia requerida para asegurar el rebaje y las galerías en muros de la zona de no interacción en minería subterránea con base en el Índice de Resistencia Geológica

RESUMEN

En la mina de cobre de Bakibaba se utiliza el método de minería por perforación de barrenos largos para extraer el mineral. Los problemas de estabilidad han ocurrido generalmente en las galerías en muro debido a la interacción entre la galería y el rebaje. En este estudio se propone un método para la estimación de la distancia mínima necesaria para asegurar la zona de no interacción entre la galería en muro y el rebaje. Se utilizó como parámetro el método del elemento finito y varias distancias entre la galería en muro y el rebaje y los desplazamientos sobre las galerías. También se realizaron análisis con varios índices de resistencia geológica de abajo hacia arriba para determinar el efecto de la masa rocoa en la interacción entre la galería en muro y el rebaje.

Palabras clave: galería en muro; análisis numérico; estabilidad subterránea.

Record
Manuscript received: 24/04/2018
Accepted for publication: 24/08/2018

How to cite item
Ozdogan, M. V., & Gonen, A. (2019). Determination of Distance Required to Ensure Stope and Footwall-drift Non-interaction Zone based on Geological Strength Index. *Earth Sciences Research Journal*, 23(1), 17-25.
DOI: https://doi.org/10.15446/esrj.v23n1.71879

ISSN 1794-6190 e-ISSN 2339-3459

https://doi.org/10.15446/esrj.v23n1.71879

Introduction

The stability of the openings in underground mines is a major factor affecting mining safety and sustainability. As such, safety and economic restrictions are the main design parameters considered in underground excavations. The geometry of an underground opening (shape and size), toe between openings and length of openings are functions of safety and cost. Decisions regarding these mining parameters are generally empirically based and at times unexpected failures occur.

The distance between the footwall drift and the stope is an important factor that affects the stability of the footwall drift. The strength of the rockmass and the mining depth significantly influence the distance required between the footwall drift and stope. In deep mines, the rockmass is highly stressed and stability problems occur around underground openings.

Although several studies have addressed the interaction between underground tunnels (Ghaboussi & Ranken, 1977, Jamshid & Randall, 1977; Yamaguchi et al. 1998; Addenbrooke & Potts, 2001; Gercek, 2005; Karakus et al. 2007; Wang et al., 2007; Wang & li, 2008; Chakeri et al. 2011; Wang et al., 2017), few have addressed the influence of the stope on the footwall drift in underground mines. Abdellaha et al. (2011) examined the interaction between the haulage drift and mine stope in a sublevel-stoping mine. The authors considered six excavation sequences in one stope and evaluated the support required for the haulage drift after each excavation. Purwanto et al. (2013) studied the influence of stope design on the stability of the hanging wall decline in cut-and-fill mines. The authors numerically analysed the stability of the hanging wall decline for various stope geometries. Kabwe & Bowa (2016) investigated the effect of the mining method on the stability of the footwall drift for the same orebody by numerically modelling the stress distribution over the stope and footwall drift for three different mining methods. On the other hand, none of the studies mentioned above have effort on determination of non-influenced zone distance between stope and footwall drift in longhole stoping mines.

The main scope of this paper is to estimate the distance between the footwall drift and stope that is necessary to ensure the existence of a non-interaction zone in longhole stoping mines. We also consider the effect of geotechnical conditions. In our study, we examined the footwall drift of the Bakibaba underground copper mine, which has experienced stability problems, and we used numerical analyses to determine the displacements over the footwall drift for various geological strength index (GSI) values..

Mining Method

The Bakibaba underground copper mine is located in Kure province in north-western Turkey, near the city of Kastamonu and the Black Sea. In this mine, a longhole-stoping and post-backfill method is used and the mine has an annual production capacity of 1,000,000 tonnes. The orebody lies in a north-easterly direction, is 100–300 m in length and averages 40 m in width. The ore deposit is 500 m in depth and the dip of the ore is 70°. The orebody is accessed via a 15% declining ramp. A footwall drift running parallel to the orebody is 5-m wide by 5-m high. Crosscuts are driven from the footwall across the orebody to the vein. The footwall drifts are positioned 40–50 m from where the footwall makes contact with the orebody. From the boundary of the ore deposit, 7-m wide by 5-m high sill drifts are driven until contact is made with the hanging wall. The upper and lower sill drifts are connected at 15-m intervals by a slot raise, and then widen to a 7-m drift width. Parallel blast holes 76 mm in diameter are drilled downward between two sill drifts. After blasting, a remote-controlled load-haul-dump (LHD) vehicle is used to muck the ore from the lower sill drift and transport it to the ore pass. After the entire stope is mined, the open stope is backfilled from the upper sill. In the Bakibaba underground mine, primary stopes are paste-filled or cemented-rock-filled and secondary stopes are rock-filled. Figure 1 shows schematic illustrations of the stope production cycle.

Numerical Model

In the mining industry, the numerical finite element method (FEM) is widely used to solve geotechnical problems. FEM can accommodate material heterogeneity, non-linear deformability, complex boundary conditions, in-situ stresses and gravity (Jing & Hudson, 2002; Sharma, 2009). The utilisation

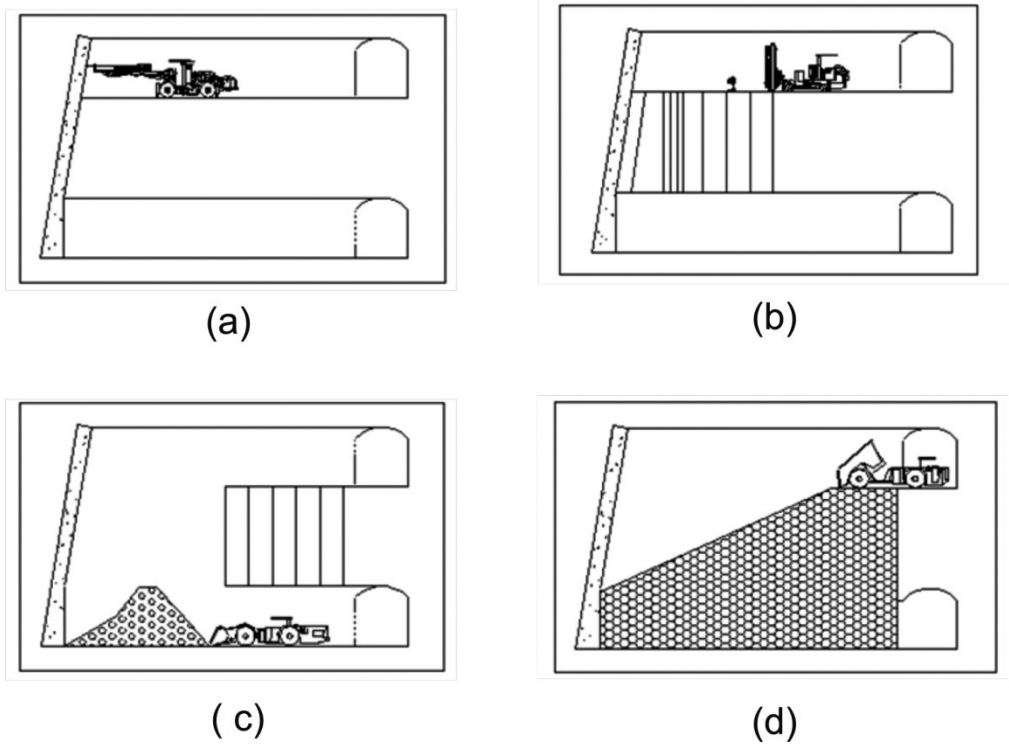

Figure 1. Stope production cycle (a: stope development, b: production drilling, c: ore mucking, d: backfilling

of FEM-based software is one of the most preferred methods, particularly in underground design analyses (Ozdogan et al. 2017). In this study, Phase² two-dimensional (2D) FEM software program developed by Rocscience (2007) was used to determine the influence of the distance between the stope and the footwall drift.

Figure 2 shows the model used in our analysis, in which we used 10-m-interval distances between the footwall drift and stope up to the stabilisation of the displacement over the drift.

Laboratory tests in accordance with ISRM standards were performed to determine the geomechanical properties of the rock unit, including the uniaxial compressive strength, unit weight, Young's modulus, Poisson's ratio, cohesion and internal friction angle of the rock unit (Table 1). To determine the rock-mass input parameters for the FEM analyses, we performed both laboratory and field studies and used Hoek and Brown criteria.

Hoek and Brown criteria developed by Hoek et al. 2002, is an empirical method to determine the strength of rock masses in terms of major and minor principal stresses and widely used criterion in geotechnical projects. Hoek and Brown criteria estimates the strength envelopes determined from laboratory triaxial tests of intact rock by using, uniaxial compressive strength of intact rock (sigci), the intact rock parameter (mi), the geological strength index (GSI) and the disturbance factor (D). The Hoek and Brown criteria is expressed as;

$$\sigma_1' = \sigma_3' + \sigma_{ci}\left(m_b \frac{\sigma_3'}{\sigma_{ci}} + s\right)^a \quad (1)$$

Where, $\sigma_{ci,}$ is the uniaxial compressive strength and m_b is the reduced value of material constant m_i which is calculated as;

$$m_b = m_i \ exp\left(\frac{GSI - 100}{28 - 14D}\right) \quad (2)$$

s and a are constants for rock mass given by;

$$s = exp\left(\frac{GSI - 100}{9 - 3D}\right) \quad (3)$$

$$a = \frac{1}{2} + \frac{1}{6}\left(e^{\frac{-GSI}{15}} - e^{\frac{-20}{3}}\right) \quad (4)$$

In order to determine rock mass parameters from laboratory test results RocData software was used. Table 2 shows the strength parameters of the rock mass derived from our laboratory and field studies. Also using a chart derived by Sheorey (1994), we calculated a total stress ratio of 1.25 for the Bakibaba Copper Mine, based on the elasticity modulus and depth.

Results and discussion

FEM analyses were performed to investigate the effect of the distance between the extracted stope and the footwall drift on drift stability, and examined various distances between them.

Table 1. Test results for rock units

Parameter, symbol, unit	Basalt (hanging wall & footwall)	Ore Zone
Unit weight, δ, kN/m³	28.04	28.80
Uniaxial compressive strength, σ_c, MPa	50.48	60.28
Brazilian tensile strength, σ_t, MPa	4.88	5.25
Young's modulus, E_i, GPa	12520	14280
Poisson's ratio, ν	0.25	0.24
Cohesion, c, MPa	9.82	10.16
Internal friction angle, Φ, °	44.5	43.25

Table 2. Input parameters used in FEM analysis

Parameters, symbol, unit	Basalt (hanging wall & footwall)	Ore Zone
Geological Strength Index (GSI)	55	60
Rock type, mi	20	20
Disturbance factor, D	0	0
Cohesion of rock mass, c, MPa	3.29	3.95
Internal friction angle of rock mass, Φ, °	38	48
Tensile strength of rock mass, σ_t, MPa	0.08	0.10
Rock mass deformation modulus, E_i, MPa	9429	10329

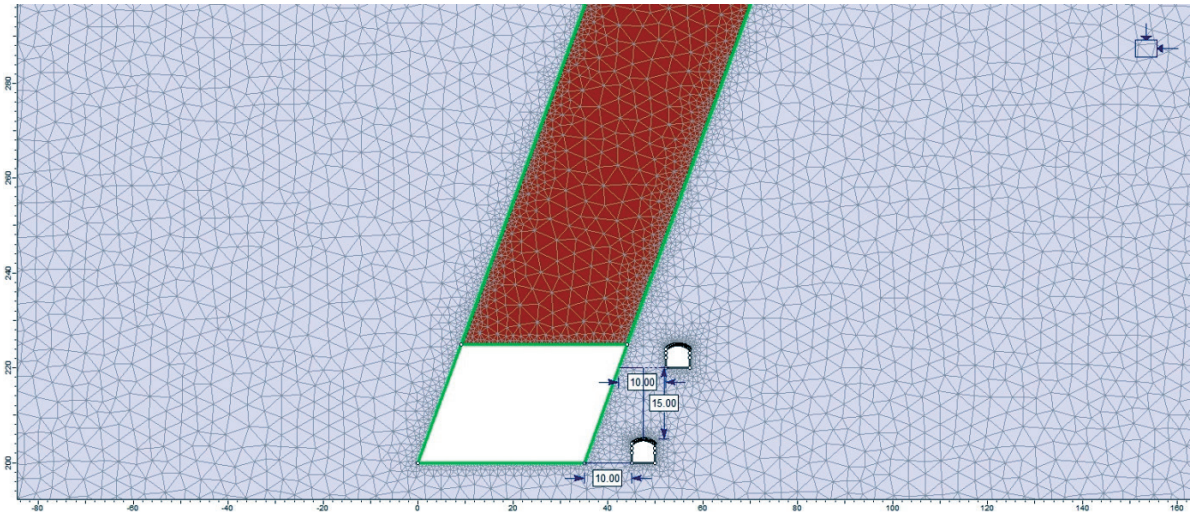

Figure 2. Base model used in analyses

Two evaluation criteria, including the yield zone, i.e. failure area, and the displacement over the footwall drift were considered. The analyses were stopped when the displacements over the drift had not changed in two consecutive analyses.

The red zones in Figure 3 indicate the 100% yield zone around underground spaces due to mining extraction when the distance from the stope to the footwall drift is 10 m. In Figure 4, the numbers on left-side wall (LW), right-side wall (RW) and roof (RF) of the drift indicate the displacement that occurred over the drift for a 10-m distance between the stope and footwall drift.

Similarly, Figures 5–7 show the changes in the yield zone and displacements for greater distances between the stope and footwall drift.

As expected, as the distance between the stope and footwall drift increases, the yield zone and displacements over drift decrease. When the distance is 10 m or less, the yield zone of the stope and footwall drift overlap and unstable drifts occur.

The model results show that when the distance between the stope and footwall drift is 10 m, the displacement on the roof of the upper drift is 0.021 m and that of the bottom drift is 0.048 m. The displacement on the roof decreases to 0.015 m for the upper drift and 0.033 m for the bottom drift for a distance of 20 m. Table 3 shows the change in the displacements over the footwall drift, in which we can see that when the distance between stope and the footwall drift is 70 m, the footwall drift is totally removed from the influence zone. Figure 8 shows the relation between distance between the stope and footwall drift and the displacements over the footwall drift.

Our numerical analyses indicate that, for the given geotechnical circumstances, the displacements over the drift become stable when there is a distance of 70 m from the stope. We conducted further numerical analyses for various GSI values to determine the effect of the GSI value on the critical distance between the stope and footwall drift. Table 4 shows the displacements around the footwall drifts for various GSI values and various stope distances. As expected, the interaction between the stope and footwall drift decreases with increases in the GSI value. However, a GSI value of 55 is the limit value regarding interaction between the stope and footwall. Higher GSI values have no influence on the non-interaction zone distance. At distances of 70 m and more between the stope and footwall drift, we observed no interaction for GSI values higher than 55. Variation of non-influenced zone distance based on GSI were shown in Figure 9.

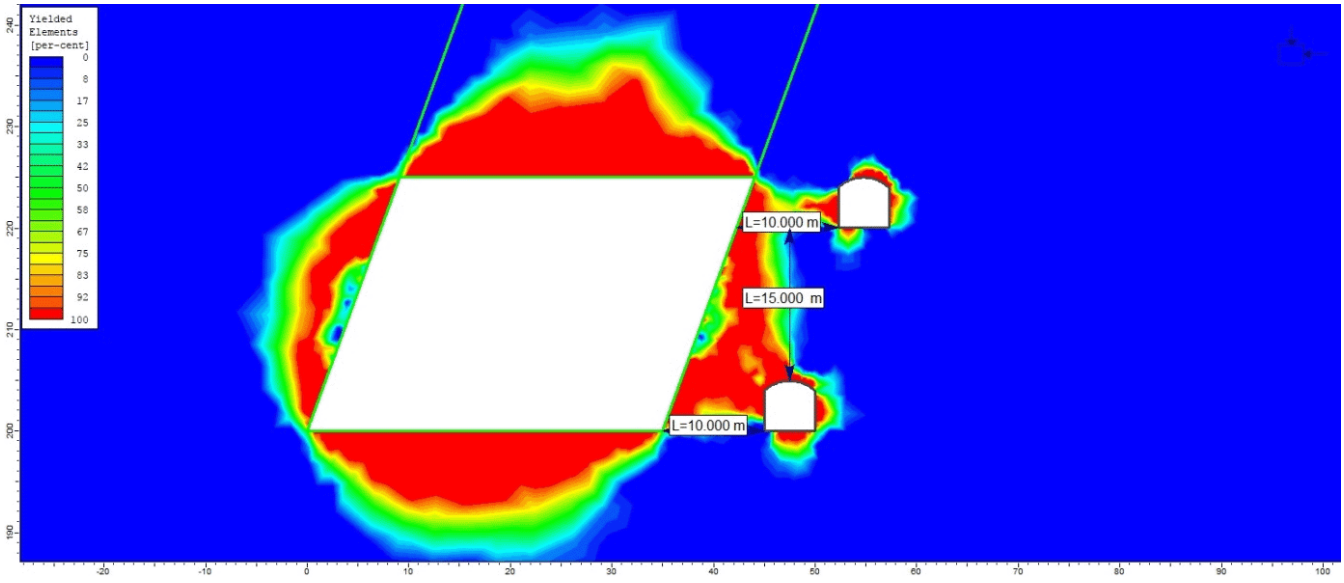

Figure 3. Yield zone for 10-m interval between stope and footwall drift

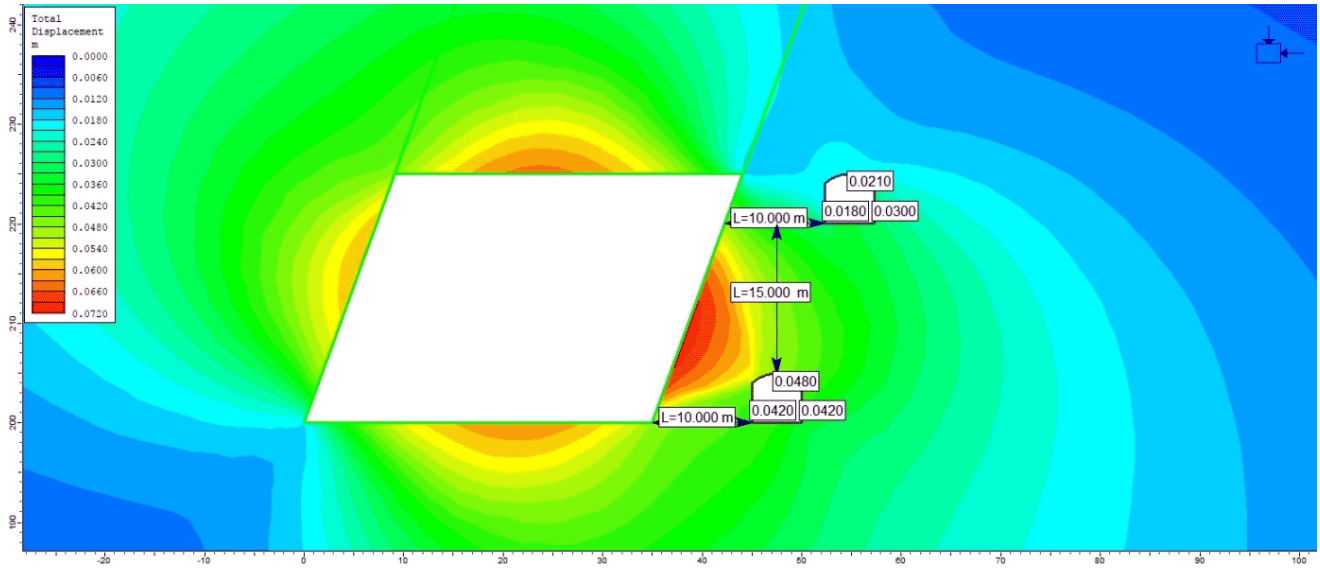

Figure 4. Displacements over footwall drift for 10-m interval between stope and footwall drift

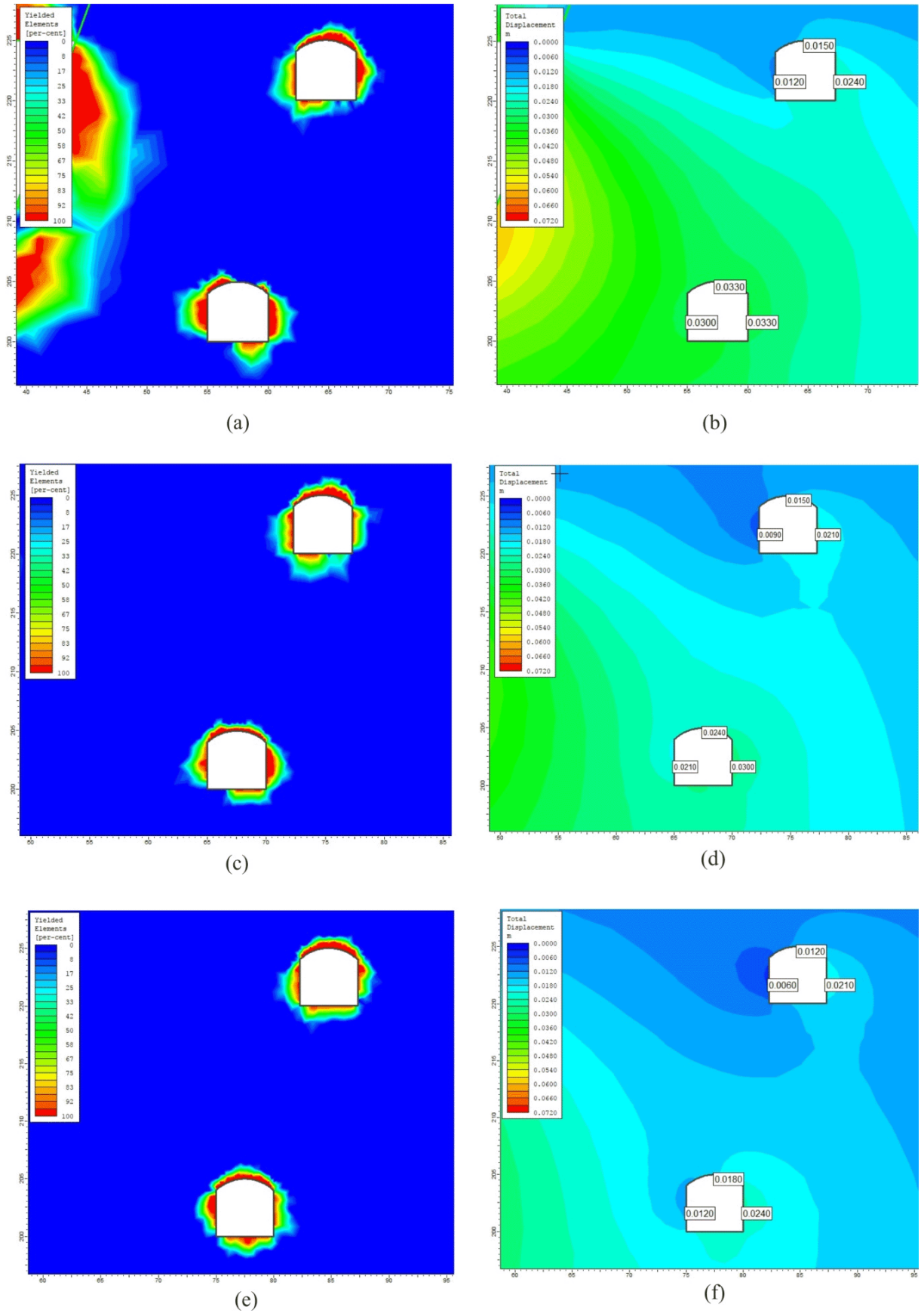

Figure 5. Yield zones and displacements for various stope–footwall-drift distances (a: yield zone for 20-m distance, b: displacements over drifts for 20-m distance, c: yield zone for 30-m distance, d: displacements over drifts for 30-m distance, e: yield zone for 40-m distance, f: displacements over drifts for 40-m distance)

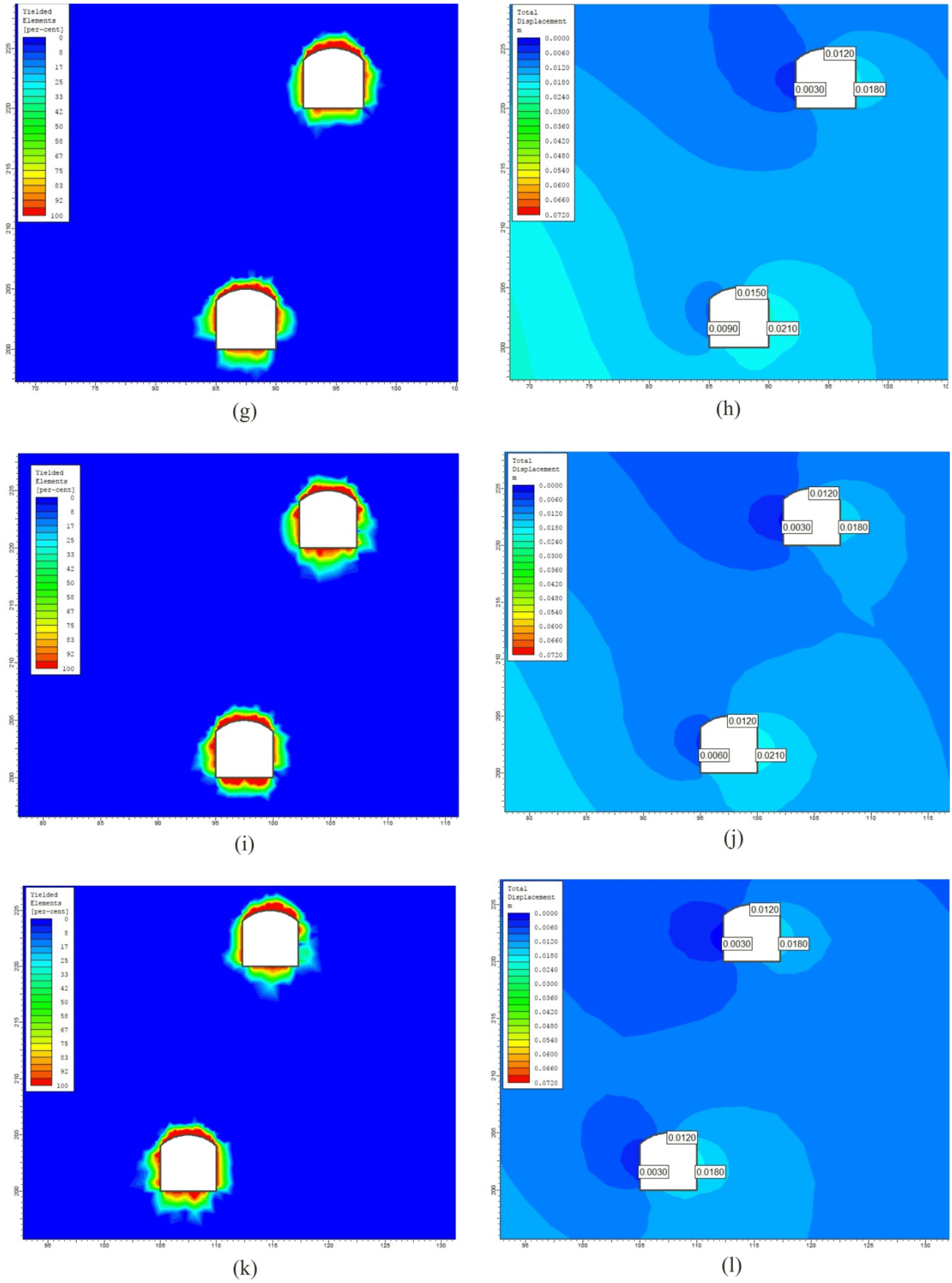

Figure 6. Yield zones and displacements for various stope–footwall-drift distances (g: yield zone for 50-m distance, h: displacements over drifts for 50-m distance, i: yield zone for 60-m distance, j: displacements over drifts for 60-m distance, k: yield zone for 70-m distance, l: displacements over drifts for 70-m distance)

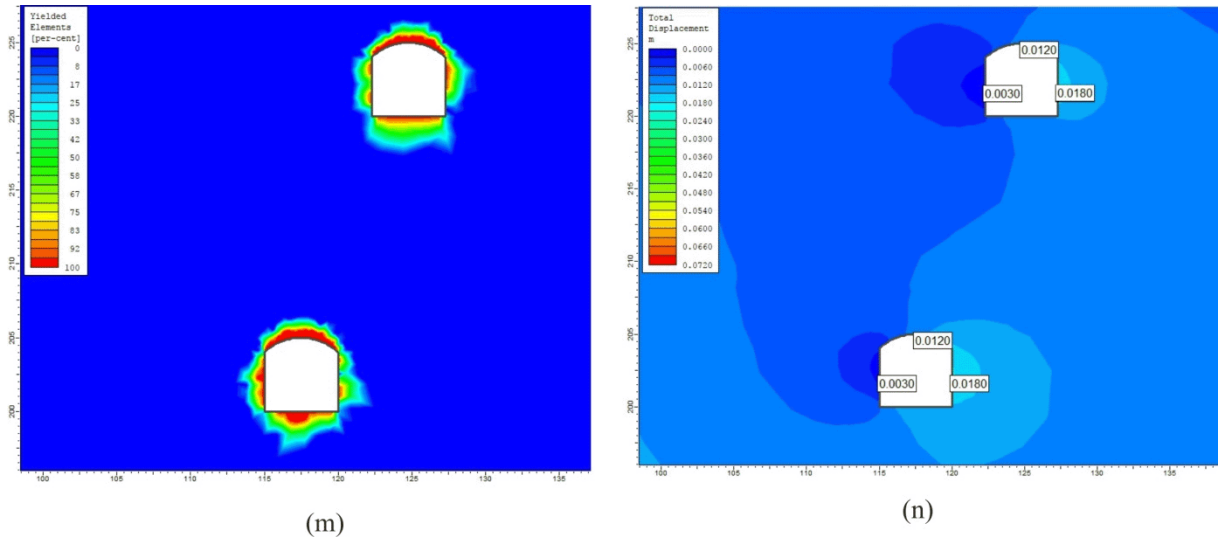

Figure 7. Yield zones and displacements for various stope–footwall-drift distances (m: yield zone for 80-m distance, n: displacements over drifts for 80-m distance)

Table 3. Change in displacements over the footwall drift

Distance between Stope and Footwall Drift (m)	Upper Drift (m)			Bottom Drift (m)		
	Left Wall	Right Wall	Roof	Left Wall	Right Wall	Roof
10	0.018	0.030	0.021	0.042	0.042	0.048
20	0.012	0.024	0.015	0.030	0.033	0.033
30	0.009	0.021	0.015	0.021	0.030	0.024
40	0.006	0.021	0.012	0.012	0.024	0.018
50	0.003	0.018	0.012	0.009	0.021	0.015
60	0.003	0.018	0.012	0.006	0.021	0.012
70	0.003	0.018	0.012	0.003	0.018	0.012
80	0.003	0.018	0.012	0.003	0.018	0.012

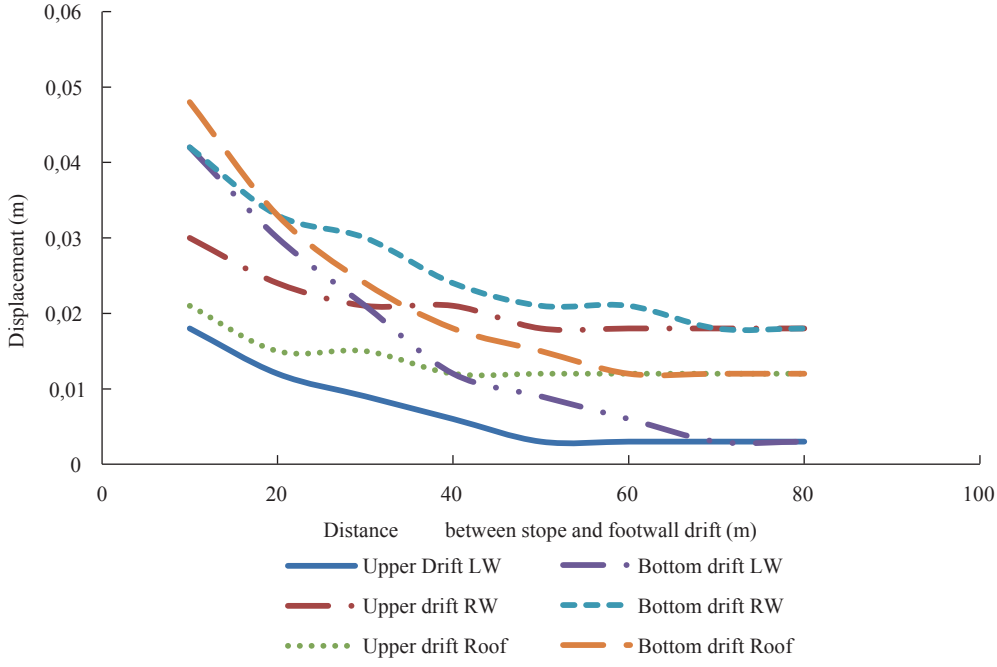

Figure 8. Relation between distance between stope and footwall drift and displacement over drift

Table 4. Displacements around footwall drifts for various GSI values and various stope distances

GSI	Distance between Stope and Footwall Drift (m)	Upper Drift (m)			Bottom Drift (m)		
		Left Wall	Right Wall	Roof	Left Wall	Right Wall	Roof
10	10	1.000	1.800	1.600	1.800	2.000	2.000
	20	0.800	1.600	1.400	0.800	1.600	1.400
	30	0.800	1.400	1.000	0.200	1.400	1.000
	40	0.600	1.200	1.000	0.400	1.200	1.000
	50	0.400	1.200	0.800	0.400	1.000	0.800
	60	0.400	1.000	0.800	0.400	1.000	0.800
	70	0.400	1.000	0.800	0.200	1.000	0.800
	80	0.200	0.800	0.600	0.200	1.000	0.600
	90	0.200	0.800	0.600	0.200	0.800	0.600
	100	0.200	0.800	0.600	0.200	0.800	0.600
35	10	0.075	0.150	0.105	0.165	0.180	0.195
	20	0.060	0.120	0.090	0.105	0.150	0.135
	30	0.045	0.105	0.075	0.075	0.120	0.105
	40	0.030	0.090	0.075	0.060	0.105	0.075
	50	0.030	0.090	0.060	0.045	0.090	0.060
	60	0.015	0.075	0.060	0.030	0.090	0.060
	70	0.015	0.075	0.060	0.015	0.090	0.060
	80	0.015	0.075	0.045	0.015	0.075	0.045
	90	0.015	0.075	0.045	0.015	0.075	0.045
55	10	0.018	0.030	0.021	0.042	0.042	0.048
	20	0.012	0.024	0.015	0.030	0.033	0.033
	30	0.009	0.021	0.015	0.021	0.030	0.024
	40	0.006	0.021	0.012	0.012	0.024	0.018
	50	0.003	0.018	0.012	0.009	0.021	0.015
	60	0.003	0.018	0.012	0.006	0.021	0.012
	70	0.003	0.018	0.012	0.003	0.018	0.012
	80	0.003	0.018	0.012	0.003	0.018	0.012
75	10	0.004	0.007	0.005	0.013	0.012	0.014
	20	0.002	0.007	0.004	0.009	0.010	0.009
	30	0.002	0.006	0.004	0.005	0.008	0.006
	40	0.001	0.005	0.003	0.004	0.007	0.005
	50	0.001	0.005	0.003	0.002	0.006	0.004
	60	0.001	0.005	0.003	0.002	0.006	0.003
	70	0.001	0.005	0.003	0.001	0.005	0.003
	80	0.001	0.005	0.003	0.001	0.005	0.003
90	10	0.002	0.003	0.002	0.006	0.005	0.006
	20	0.001	0.003	0.002	0.004	0.004	0.004
	30	0.001	0.002	0.002	0.003	0.003	0.003
	40	0.001	0.002	0.002	0.002	0.003	0.003
	50	0.001	0.002	0.001	0.001	0.003	0.002
	60	0.001	0.002	0.001	0.001	0.002	0.002
	70	0.001	0.002	0.001	0.001	0.002	0.001
	80	0.001	0.002	0.001	0.001	0.002	0.001

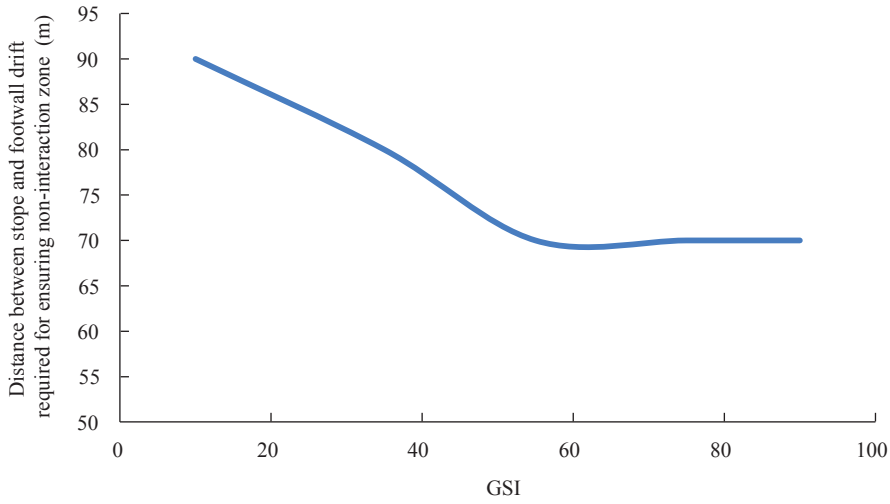

Figure 9. Variations in distance between stope and footwall based on GSI value

Conclusions

In this study, 3D finite element method was used to investigate the interaction between the stopes and footwall drifts of the Bakibaba underground copper mine. We determined the range of influence between the stope and footwall drift for the currently existing circumstances. Then, the GSI value was systematically increased while keeping all the other parameters constant to determine the effect of the GSI value on this range of influence. Our series of numerical simulations revealed that a distance of 70 m is necessary to ensure the existence of a non-interaction zone between the stope and footwall drift at the Bakibaba Copper Mine. Our analyses also show that the GSI value of the rock mass has a significant effect on this non-interaction zone distance up to a GSI value of 55, after which higher GSI values do not increase the required non-interaction-zone distance..

References

Abdellaha, W., Mitria, H., & Thibodeau, D. (2011). Assessment of Mine Haulage Drift Safety Using Probabilistic Methods of Analysis. *Procedia Engineering, 26,* 2099–2111. DOI: https://doi.org/10.1016/j.proeng.2011.11.2412

Addenbrooke, T. I., & Potts, D. M. (2001). Twin tunnel interaction: surface and subsurface effects. *International Journal of Geomechanics*, 1(2), 249–271

Chakeri, H., Hasanpour, R., Hindistan, M. A., & Unver, B. (2011). Analysis of interaction between tunnels in soft ground by 3D numerical modeling. *Bulletin of Engineering Geology and the Environment*, 70, 439–448. DOI: http://dx.doi.org/10.1007/s10064-010-0333-8

Gercek, H. (2005). *Interaction between Parallel Underground Openings*. The 19th International Mining Congress and Fair of Turkey, IMCET

Ghaboussi, J. & Ranken R. E. (1977). Interaction between Two Parallel Tunnels. *International Journal for Numerical and Analytical Methods in Geomechanics*, 1(1), 75-103. DOI: https://doi.org/10.1002/nag.1610010107

Hoek, E., Carranza-Torres, C. & Corkum, B. (2002). *Hoek-Brown Failure Criterion- 2002 Edition*. Proceedings NARMAS-TAC Conference, Toronto, 1,267-273

Jing, L., & Hudson, J. A. (2002). Numerical methods in rock mechanics. *International Journal of Rock Mechanics and Mining*, 39, 409–427.

Kabwe, E., & Bowa, V. M. (2016). Determination of the Appropriate Geometry of Footwall Drifts Using Numerical Analysis Technique. *Geotechnical and Geological Engineering*, 34, 1955–1969. DOI: https://doi.org/10.1007/s10706-016-0076-9

Karakus, M., Ozsan, A., & Basarir, H. (2007). Finite element analysis for the twin metro tunnel constructed in Ankara Clay-Turkey. *Bulletin of Engineering Geology and the Environment*, 66, 71–79. DOI: http://dx.doi.org/10.1007/s10064-006-0056-z

Ozdogan, M. V, Yenice, H., Gonen, A., & Karakus, D. (2017). Optimal Support Spacing for Steel Sets: Omerler Underground Coal Mine in Western Turkey. International Journal of Geomechanics, 18(2), 05017003-1-12. http://dx.doi.org/10.1061/(ASCE)GM.1943-5622.0001069

Purwanto, A., Shimada, H., Sasaoka, T., Wattimena, R. K., & Matsui, K. (2013). Influence of Stope Design on Stability of Hanging Wall Decline in Cibaliung Underground Gold Mine. *International Journal of Geosciences,* 4, 1-8. DOI: http://dx.doi.org/10.4236/ijg.2013.410A001

Sharma, K. G. (2009). Numerical analysis of underground structures. *Indian Geotechnical Journal*, 39(1), 1–63

SheoreyP.R.(1994).Atheoryforinsitustressesinisotropicandtransverselyisotropic rock. *International Journal of Rock Mechanics and Mining Sciences*, 31(1), 23-34. DOI: https://doi.org/10.1016/0148-9062(94)92312-4

Wang, B., & Li, S. (2008). A complex variable solution for stress and displacement field around a lined circular tunnel at great depth. *International Journal for Numerical and Analytical Methods in Geomechanics*, 33, 939-951. DOI: https://doi.org/10.1002/nag.749

Wang, H. N., Zenga, G. S., Utilic, S., Jiangd, M. J., & Wua, L. (2017). Analytical solutions of stresses and displacements for deeply buried twin tunnels in viscoelastic rock. *International Journal of Rock Mechanics & Mining Sciences,* 93, 13–29. DOI: https://doi.org/10.1016/j.ijrmms.2017.01.002

Wang, J., Milne, D., Wegner, L. & Reeves, M. (2007). Numerical Evaluation of the Effects of Stress and Excavation Surface Geometry on the Zone of Relaxation around Open Stope Hanging Walls. *International Journal of Rock Mechanics & Mining Sciences*, 44(2), 289-298. DOI: http://dx.doi.org/10.1016/j.ijrmms.2006.07.002

Yamaguchi, I., Yamazaki, I., & Kiritani, K. (1998). Study of ground-tunnel interactions of four shield tunnels driven in close proximity, in relation to design and constructions of parallel shield tunnels. *Tunnelling and Underground Space Technology,* 13(3):289–304. DOI: https://doi.org/10.1016/S0886-7798(98)00063-7